• Letter to the Editor •

Imaging of retinal nerve fiber in non-arteritic anterior ischemic optic neuropathy at acute, sub-acute, and chronic phases: adaptive optics scanning laser ophthalmoscopy versus optical coherence tomography

Yi Gong, Shuo Sun, Rong Luan, Bo-Shi Liu, Rong-Guo Yu, Xiao-Rong Li

Tianjin Key Laboratory of Retinal Functions and Diseases, Tianjin Branch of National Clinical Research Center for Ocular Disease, Eye Institute and School of Optometry, Tianjin Medical University Eye Hospital, Tianjin 300384, China
Co-first Authors: Yi Gong and Shuo Sun
Correspondence to: Rong-Guo Yu and Xiao-Rong Li. Tianjin Medical University Eye Hospital, 251 Fu Kang Road, Tianjin 300384, China. 13820179302@163.com; xiaorli@163.com
Received: 2025-02-21 Accepted: 2025-08-11

DOI:10.18240/ijo.2026.06.22

Citation: Gong Y, Sun S, Luan R, Liu BS, Yu RG, Li XR. Imaging of retinal nerve fiber in non-arteritic anterior ischemic optic neuropathy at acute, sub-acute, and chronic phases: adaptive optics scanning laser ophthalmoscopy versus optical coherence tomography. *Int J Ophthalmol* 2026;19(6):1201-1205

Dear Editor,

Non-arteritic anterior ischemic optic neuropathy (NAION) is the most common acute optic neuropathy in individuals over 50 years old, characterized by a sudden, painless, monocular vision loss or variable visual field defect with optic disc edema[1]. Although the exact pathogenesis of NAION remains uncertain, optic disc swelling and nerve compression results in axonal damage and retinal ganglion cell apoptosis[2]. Retinal nerve fiber layer (RNFL) defect detection is essential for diagnosing and managing NAION. The RNFL loss could be detected and evaluated by optical coherence tomography (OCT) and various other imaging techniques[3]. Nonetheless, none of these modalities have the necessary lateral resolution to visualize individual RNFL bundles, largely due to aberrations in ocular optics.

Adaptive optics (AO) system improves image quality by compensating for the aberrations in optical system[4]. Combining AO system with other imaging modalities including flood-illuminated ophthalmoscopy, OCT and scanning laser ophthalmoscopy (SLO) have allowed for visualization of the individual cone photoreceptors, RNFL bundles and blood cells[5-6].

The purpose of this study was to better understand RNFL bundle loss in patients with NAION at different stages using AO-SLO imaging. This is the first case reports investigating the RNFL bundle loss over time in NAION using AO-SLO.

CASE REPORT

Ethical Approval The study involving human participants was reviewed and approved by Ethics Committee of Tianjin Medical University Eye Hospital (2022KY-18) and was performed in accordance with the ethical standards laid down by the Declaration of Helsinki. The patients/participants provided their written informed consent to participate in this study. Written informed consent was obtained from the individual(s) for the publication of any potentially identifiable images or data included in this article.

Three patients with NAION at different stages admitted to Tianjin Medical University Eye Hospital were tested. The clinical features of the patients are summarized in Table 1. AO-SLO images (Mona II, Robotrak Technologies, Nanjing, China) were obtained of retinal nerve fiber bundles near the temporal region of the optic disc margin. After the features were located and in focus, images were captured using a 5° square field of view. Circumpapillary OCT scans and optical coherence tomography angiography (OCTA) were obtained for all eyes using swept-source OCT (VG200S; SVision Imaging, Henan, China). The widths of the hyperreflective bundles in AO-SLO images of the 3 eyes can be seen in Figures 1-3, which were clearly differed at various time points.

Case 1 A 31-year-old male presented with a 14-day history of sudden, painless, and progressively worsening blurred vision in his left eye. Nine months earlier, he had experienced a similar episode in his right eye that was diagnosed as NAION. Fundoscopic examination revealed hyperemic optic disc swelling in the acutely affected left eye and optic disc pallor in the right eye, consistent with prior NAION. The patient denied symptoms suggestive of giant cell arteritis, and laboratory investigations, including inflammatory markers,

Table 1 Clinical characteristics of the patients

Characteristics	Patient 1 (acute)	Patient 2 (sub-acute)	Patient 3 (chronic)
Age, y	31	61	55
Gender	Male	Male	Female
Duration, d	14	45	65
Affected eye	OS	OD	OS
C/D	0	0	0
C/D (contralateral eye)	0.69	0.07	0
BCVA, logMAR	0.82	0.52	0.70
IOP, mm Hg	10.4	18.2	11.0
Average RNFL thickness, μm	235	193	80
Axial length, mm	23.26	22.65	20.73
Prior treatments	None	Oral vasodilator (calcium dobesilate and compound Xueshuantong)	Oral steroids, superficial temporal artery injection of compound anisodine hydrobromide injection

C/D: Cup/disc; BCVA: Best corrected visual acuity; IOP: Intraocular pressure; RNFL: Retinal nerve fiber layer; logMAR: Logarithm of the minimal angle of resolution; OD: Right eye; OS: Left eye.

were unremarkable. Contrast-enhanced magnetic resonance imaging (MRI) of the brain and orbits showed no structural abnormalities. In patient 1, the nerve fibers surrounding the optic disc were swollen, and the widths of the hyperreflective bundles ranged from 20.9 to 32.0 μm, with a median of 26.0 μm and an interquartile interval from 21.3 to 30.5 μm (Figure 1B). AO-SLO image showed high-contrast RNFL, which were associated with abnormally thick RNFLs on the circumpapillary circle scan of OCT (Figure 1C-1F).

Case 2 A 61-year-old male presented with a 45-day history of sudden, progressive, painless visual blurring in his right eye. Serial fundus examinations revealed an evolving pattern of optic disc edema-initial imaging documented superior sectoral disc swelling at disease onset, while current evaluation demonstrated new inferior sectoral disc swelling in the same eye. Systemic evaluation showed normal blood pressure and unremarkable laboratory findings, with no clinical evidence of giant cell arteritis. In patient 2 (Figure 2B), the retinal nerve fiber bundles in the inferior region of AO-SLO image seem within normal limits, which ranged from 8.9 to 13.1 μm (median: 9.6 μm, interquartile interval: 9.5-10.4 μm), comparing with the superior region (ranged from 12.6 to 24.2 μm, median: 19.0 μm, interquartile interval: 17.7-20.3 μm). In the case of patient 2, bundles with markedly reduced contrast were seen in the inferior region of AO-SLO. And it was consisted with the value of RNFL thickness (Figure 2F).

Case 3 A 55-year-old female presented with a 65-day history of sudden, progressive and painless visual blurring in her left eye, accompanied by a superior altitudinal visual field defect. Ophthalmic evaluation confirmed the diagnosis of NAION in the left eye. Funduscopic examination revealed optic disc pallor in the right eye, suggestive of prior ischemic damage. The patient denied any symptoms consistent with giant cell arteritis, and inflammatory markers were within normal limits. In patient 3 (Figure 3B), there had reasonably large region with an apparent loss of retinal nerve fiber bundles as indicated by the red arrows and the remaining nerve fibers were thinner than that in the acute and sub-acute stage (ranged from 5.2 to 10.3 μm, median: 8.1 μm, interquartile interval: 5.7-10.5 μm). There were relatively large regions devoid of bundles throughout the temporal area (Figure 3B, red arrows). And as mentioned above, several abnormal-appearing bundles were also seen among the AO-SLO regions. In general, it fell within the abnormal range of the RNFL thickness plot (Figure 3C-3F). However, the RNFL thickness in these regions of missing nerve bundles demonstrated in B-scan was not zero (Figure 4).

DISCUSSION

The typical symptom of acute NAION is optic disc edema resulting from blocked axoplasmic flow and axonal injury. This condition often shows spontaneous improvement within weeks, accompanied by apoptosis of ganglion cell bodies. Consequently, non-functional swelling of axons diminishes progressively, leading to their shrinkage and thinning over time[7].

Regarding the progression of NAION, it is often difficult to determine whether the reduction in optic disc edema is due solely to the nerve fiber recovery or loss of axons and viable retinal ganglion cells. Clinically, the prevailing trend manifests as progressive atrophy characterized by RNFL loss and thinning and generalized or sectoral atrophy of the optic disc. The measurement of circumpapillary RNFL thickness is a widely utilized method in clinical practice to assess morphological changes of RNFL, including swelling and atrophy, in patient with NAION.

AO equipment compensates for the aberrations of eyes and is capable of resolving single cells in the living retina, therefore providing the opportunity to identify individual photoreceptors, microvasculature and vascular flow[8-10]. Moreover, AO-SLO images have demonstrated normal, within normal limits and abnormal nerve fiber bundles in both control and

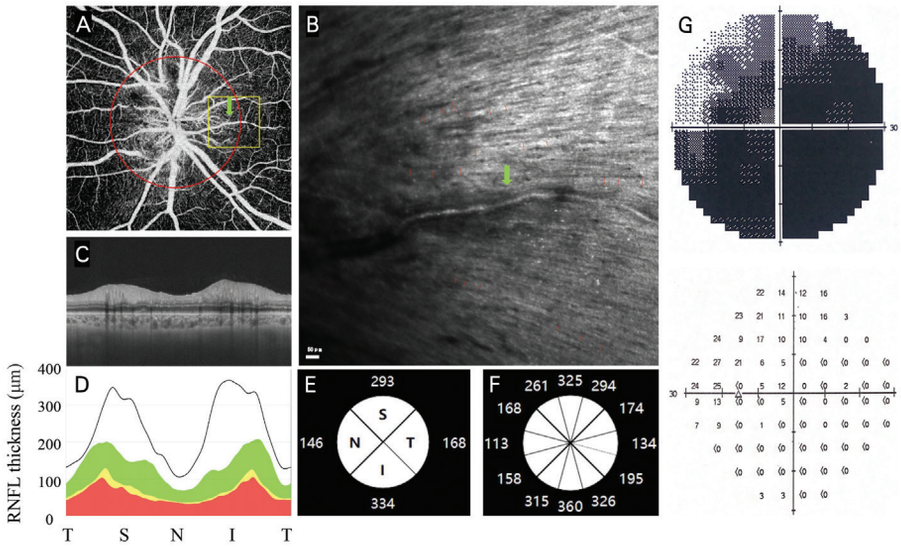

Figure 1 Example of multimodal retinal imaging in a 31-year-old male patient diagnosed with acute NAION A: Swept-source OCTA image of radial peripapillary capillary layer with the yellow square indicated the same field of view with AO-SLO. Red circle showed the scan for the patient obtained along the circumpapillary path, 3.4 mm in diameter; B: AO-SLO image at temporal of the disc. The green arrow seen on the OCTA images of radial capillary layer and AO-SLO images indicate the same blood vessels. These landmarks allow us to locate corresponding area on the AO-SLO and OCT B-scan; C: Circumpapillary circle scan from temporal (T) to superior (S) to nasal (N) to inferior (I) to T regions; D: A TSNIT RNFL thickness plot. The value of RNFL thickness were automatically divided into 4 (E) and 9 orientations (F); G: Visual field showed a small residual superior temporal field. Scale bar: in (B) was 50 μm. NAION: Non-arteritic anterior ischemic optic neuropathy; OCTA: Optical coherence tomography angiography; AO-SLO: Adaptive optics-scanning laser ophthalmoscopy; OCT: Optical coherence tomography; RNFL: Retinal nerve fiber layer.

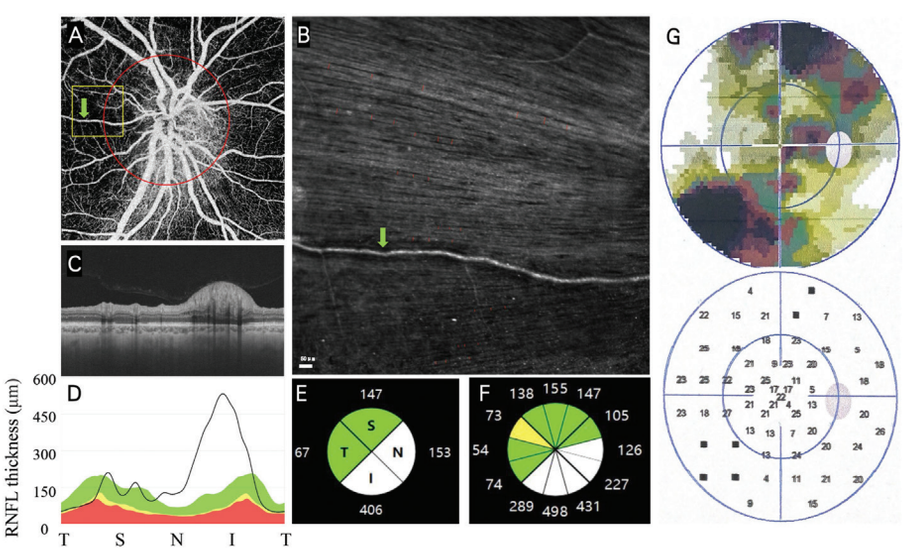

Figure 2 Example of multimodal retinal imaging in a 61-year-old male patient diagnosed with sub-acute NAION A: Swept-source OCTA image of radial peripapillary capillary layer with the yellow square indicated the same field of view with AO-SLO. Red circle showed the scan for the patient obtained along the circumpapillary path, 3.4 mm in diameter; B: AO-SLO image at temporal of the disc. The green arrow seen on the OCTA images of radial capillary layer and AO-SLO images indicate the same blood vessels. These landmarks allow us to locate corresponding area on the AO-SLO and OCT B-scan; C: Circumpapillary circle scan from temporal (T) to superior (S) to nasal (N) to inferior (I) to T regions; D: A TSNIT RNFL thickness plot. The value of RNFL thickness were automatically divided into 4 (E) and 9 orientations (F); G: Visual field showed inferior nasal and superior temporal defect and was connected to the optic disc. Scale bar: in (B) was 50 μm. NAION: Non-arteritic anterior ischemic optic neuropathy; OCTA: Optical coherence tomography angiography; AO-SLO: Adaptive optics-scanning laser ophthalmoscopy; OCT: Optical coherence tomography; RNFL: Retinal nerve fiber layer.

glaucomatous eyes[11-14]. Given its sensitivity and objectivity in detecting structural changes, the integration of AO-SLO into a multimodal imaging system may be imperative for advancing NAION clinical trials. However, AO-SLO is not ready and

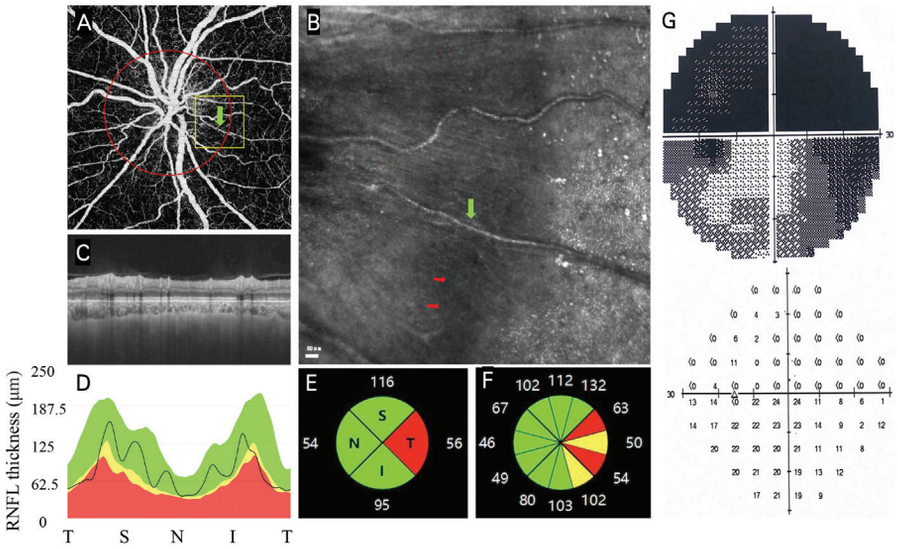

Figure 3 Example of multimodal retinal imaging in a 55-year-old female patient diagnosed with chronic NAION A: Swept-source OCTA image of radial peripapillary capillary layer with the yellow square indicated the same field of view with AO-SLO. Red circle showed the scan for the patient obtained along the circumpapillary path, 3.4 mm in diameter; B: AO-SLO image at temporal of the disc. The green arrow seen on the OCTA images of radial capillary layer and AO-SLO images indicate the same blood vessels. These landmarks allow us to locate corresponding area on the AO-SLO and OCT B-scan. There were relatively large regions devoid of bundles throughout the temporal area (red arrows); C: Circumpapillary circle scan from temporal (T) to superior (S) to nasal (N) to inferior (I) to T regions; D: A TSNIT RNFL thickness plot. The value of RNFL thickness were automatically divided into 4 (E) and 9 orientations (F); G: Visual field showed a superior altitudinal defect and was connected to the optic disc. Scale bar: in (B) was 50 μm. NAION: Non-arteritic anterior ischemic optic neuropathy; OCTA: Optical coherence tomography angiography; AO-SLO: Adaptive optics-scanning laser ophthalmoscopy; OCT: Optical coherence tomography; RNFL: Retinal nerve fiber layer.

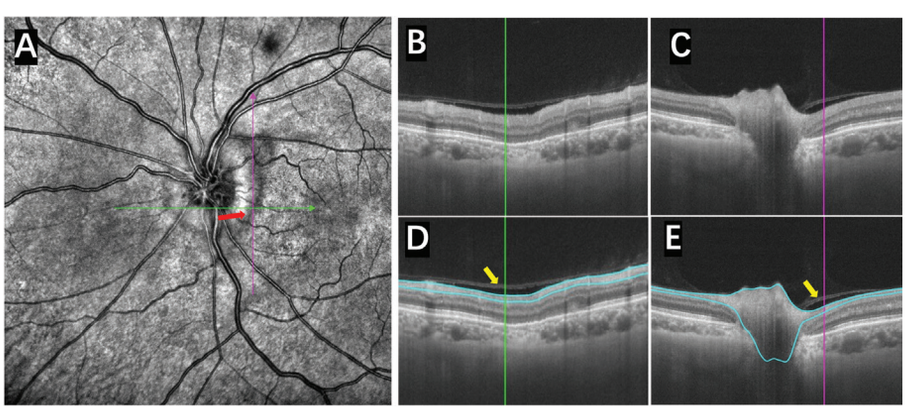

Figure 4 Comparison of multimodal retinal imaging in RNFL A: Swept-source OCTA en-face image of optic disc. Red arrow illustrated region lack of retinal nerve fiber bundles in patient 3; B-C: B-scan retina images of the vertical line (purple) and horizonal line (green) in A; D-E: RNFL borders were marked automatically. Yellow arrows showed the OCT RNFL thickness was not zero, but was approximately 50 μm thick. RNFL: Retinal nerve fiber layer; OCTA: Optical coherence tomography angiography; OCT: Optical coherence tomography.

convenient for routine clinical use. First, it is difficult to get acceptable images on patients with cataracts, high refractive error or small pupils. Second, there are lack of standardized terminology and measurement parameters of AO devices. Finally, AO-SLO is limited spatially by a small field of view and the montaging is time consuming.

The purpose of our study was to describe the characteristics of acute, sub-acute and chronic NAION in terms of retinal nerve fiber loss as seen with AO-SLO. The AO-SLO images of these eyes with abnormal width (swollen or thin) of retinal nerve fibers approximately reflected the same with circumpapillary thickness plot. However, due to its better transverse resolution compared to swept-source OCT, it allowed for detailed visualization of the individual nerve fibers, including the edge of abnormal bundles. Furthermore, in regions where AO-SLO images displayed no discernible retinal nerve fiber bundles, the OCT measurement of RNFL thickness did not register as zero, consistent with findings from Hood DC's

study on glaucoma[15]. The residual OCT thickness might include less intense structures (*e.g.*, retinal ganglion cell and inner plexiform layer) by automatic segmentation errors, the end feet of the Müller cells and non-functional axons. And the accuracy of angio-OCT in disc boundary detection and radial peripapillary capillary layer segmentation was reduced in acute NAION with edematous optic discs[16].

There were several limitations in our study. First, the imaging scope was limited to the temporal region of the optic disc margin, which was easy to take in a short timeframe. Second, there lacked normative databases of RNFL bundles in healthy controls detecting by AO-SLO. Third, we measured nerve fiber bundle widths manually, which was impractical for clinical use. With the development of technology and deep learning, automated segmentation software may be available in the future. In conclusion, this case series study represented the first description of AO-SLO images at different stages of NAION, further investigation is needed to explore the potential of montage AO-SLO in healthy controls and patients follow-up, particularly in detecting "subclinical" changes or assessing treatment response.

In summary, the AO-SLO images revealed details of retinal nerve fiber damage in acute, sub-acute and chronic NAION, compensating for the limitations of swept-source OCT. It enhanced visualization capacity for optimizing clinical strategies in NAION management and facilitating longitudinal assessment of disease progression.

ACKNOWLEDGEMENTS

Authors' Contributions: Study design, data acquisition and analysis: Gong Y and Sun S; Drafting the manuscript and figures: Yu RG and Luan R; Reviewing the manuscript: Sun S, Yu RG, Liu BS and Li XR.

Foundations: Supported by Tianjin Key Medical Discipline (Specialty) Construction Project (No.TJYXZDXK-3-004A-2); Science and Technology Project of Tianjin Binhai New Area Health Commission (No.2022BWKQ011); Natural Science Foundation of Tianjin City (No.22JCQNJC01220); The Science & Technology Development Fund of Tianjin Education Commission for Higher Education (No.2021KJ233).

Conflicts of Interest: Gong Y, None; **Sun S,** None; **Luan R,** None; **Liu BS,** None; **Yu RG,** None; **Li XR,** None.

REFERENCES

1 Hayreh SS. Ischemic optic neuropathy. *Prog Retin Eye Res* 2009;28(1):34-62.

2 Arnold AC. Pathogenesis of nonarteritic anterior ischemic optic neuropathy. *J Neuro Ophthalmol* 2003;23(2):157-163.

3 Aghsaei Fard M, Ghahvechian H, Subramanian PS. Follow-up of nonarteritic anterior ischemic optic neuropathy with optical coherence tomography angiography. *J Neuro Ophthalmol* 2021;41(4):e433-e439.

4 Zhang B, Li N, Kang J, *et al*. Adaptive optics scanning laser ophthalmoscopy in fundus imaging, a review and update. *Int J Ophthalmol* 2017;10(11):1751-1758.

5 Bakker E, Dikland FA, van Bakel R, *et al*. Adaptive optics ophthalmoscopy: a systematic review of vascular biomarkers. *Surv Ophthalmol* 2022;67(2):369-387.

6 Britten-Jones AC, Thai L, Flanagan JPM, *et al*. Adaptive optics imaging in inherited retinal diseases: a scoping review of the clinical literature. *Surv Ophthalmol* 2024;69(1):51-66.

7 Huang HM, Wu PC, Kuo HK, *et al*. Natural history and visual outcome of nonarteritic anterior ischemic optic neuropathy in Southern Taiwan: a pilot study. *Int Ophthalmol* 2020;40(10):2667-2676.

8 Ishikura M, Muraoka Y, Kadomoto S, *et al*. Retinal arterial macroaneurysm rupture caused by dissection-like change in the vessel wall. *Am J Ophthalmol Case Rep* 2022;25:101346.

9 Toledo-Cortés S, Dubis AM, González FA, *et al*. Deep density estimation for cone counting and diagnosis of genetic eye diseases from adaptive optics scanning light ophthalmoscope images. *Trans Vis Sci Tech* 2023;12(11):25.

10 Wynne N, Jiang YY, Aleman TS, *et al*. Retinal sensitivity in comparison to cone density in choroideremia. *Invest Ophthalmol Vis Sci* 2024;65(14):6.

11 Takayama K, Ooto S, Hangai M, *et al*. High-resolution imaging of retinal nerve fiber bundles in glaucoma using adaptive optics scanning laser ophthalmoscopy. *Am J Ophthalmol* 2013;155(5):870-881.e3.

12 Chen MF, Chui TYP, Alhadeff P, *et al*. Adaptive optics imaging of healthy and abnormal regions of retinal nerve fiber bundles of patients with glaucoma. *Invest Ophthalmol Vis Sci* 2015;56(1):674-681.

13 Hood DC, Lee D, Jarukasetphon R, *et al*. Progression of local glaucomatous damage near fixation as seen with adaptive optics imaging. *Trans Vis Sci Tech* 2017;6(4):6.

14 Choudhari NS, Kumar S, Richhariya A, *et al*. Adaptive optics scanning laser ophthalmoscopy may support early diagnosis of glaucoma. *Indian J Ophthalmol* 2022;70(8):2877-2882.

15 Hood DC, Chen MF, Lee D, *et al*. Confocal adaptive optics imaging of peripapillary nerve fiber bundles: implications for glaucomatous damage seen on circumpapillary OCT scans. *Trans Vis Sci Tech* 2015;4(2):12.

16 Anvari P, Sardarinia M, Zand A, *et al*. Accuracy of peripapillary OCTA in patients with acute nonarteritic anterior ischemic optic neuropathy. *Can J Ophthalmol* 2023;58(6):577-581.